Demarcation of a New Circulating Turbulent Fluidization Regime

Xiaobo Qi, Haiyan Zhu, and Jesse Zhu
Dept. of Chemical and Biochemical Engineering, University of Western Ontario, London, Ontario, Canada, N6A 5B9

DOI 10.1002/aic.11735
Published online January 22, 2009 in Wiley InterScience (www.interscience.wiley.com).

Transient flow behaviors in a novel circulating-turbulent fluidized bed (C-TFB) were investigated by a multifunctional optical fiber probe, that is capable of simultaneously measuring instantaneous local solids-volume concentration, velocity and flux in gas-solid two-phase suspensions. Microflow behavior distinctions between the gas-solid suspensions in a turbulent fluidized bed (TFB), conventional circulating fluidized bed (CFB), the bottom region of high-density circulating fluidized bed (HDCFB), and the newly designed C-TFB were also intensively studied. The experimental results show that particle-particle interactions (collisions) dominate the motion of particles in the C-TFB and TFB, totally different from the interaction mechanism between the gas and solid phases in the conventional CFB and the HDCFB, where the movements of particles are mainly controlled by the gas-particle interactions (drag forces). In addition, turbulence intensity and frequency in the C-TFB are significantly greater than those in the TFB at the same superficial gas velocity. As a result, the circulating-turbulent fluidization is identified as a new flow regime, independent of turbulent fluidization, fast fluidization and dense suspension upflow. The gas-solid flow in the C-TFB has its inherent hydrodynamic characteristics, different from those in TFB, CFB and HDCFB reactors. © 2009 American Institute of Chemical Engineers *AIChE J,* 55: 594–611, 2009
Keywords: circulating-turbulent fluidized bed, turbulent fluidized bed, high-density circulating fluidized bed, hydrodynamics, flow regime, circulating-turbulent fluidization

Introduction

Gas-solid fluidized beds have been widely applied in various industrial processes involving gas-solid contact, including combustion, gasification, catalytic cracking, calcinations, drying, etc.[1–4] It is well known that gas-solid fluidized beds may operate in the following flow regimes: particulate fluidization, bubbling (slugging) fluidization, turbulent fluidization, fast fluidization, dense suspension upflow and pneumatic transport. While each of these flow regimes has applications in industrial practice, most key commercial gas-solid fluidized-bed reactors operate in the flow regimes of turbulent fluidization, fast fluidization and dense suspension upflow due to their favorable gas-solid contacting, mixing and transfer characteristics.[5] Despite their advantages, such as the high throughput per unit reactor volume and independent gas/solids flow rate control in circulating fluidized beds (CFBs), the vigorous gas-solid contacting, favorable bed-to-surface heat transfer, and high-solids concentration (typically 25–35% by volume) in turbulent fluidized beds (TFBs), some inherent shortcomings of the extremely nonuniform axial and radial gas/solids distribution and low-solids concentration (usually less than 10%) in CFBs, and the intense axial solids backmixing in TFBs, limit or hinder further performance of improvement of these reactors with better gas-solid contacting efficiency and higher conversion per unit volume.[5–10] The relatively low-solids concentration and the nonuniform axial and radial-flow structure in CFBs result in a key disad-

Correspondence concerning this article should be addressed to J. Zhu at zhu@uwo.ca.

vantage, the serious gas by-passing through the core dilute region and extensive backmixing of solids in the wall region, consequently, leading to reduced overall gas-solid contact efficiency, and poor selectivity of chemical reactions.[11] Although the gas and solid phases in TFBs have much more uniform radial distributions than in CFBs, serious backmixing of the solids phases leads to a broad residence time-distribution of the solids, resulting in poor chemical reaction selectivity in TFBs, for example, for gas-phase catalytic reactions where the catalysts deactivated rapidly.

To distinguish high-flux and high-density operating conditions encountered in FCC risers from those low-flux and low-density operations corresponding to the CFB combustors, Bi and Zhu[12] proposed a concept of high-density circulating fluidized beds (HDCFBs). After that, a series of studies have been carried out to study the hydrodynamics in HDCFBs. The experimental results of Issangya et al.[13–15] have shown that under high superficial gas velocities (U_g = 4~8 m/s) and high-solids circulation rates (G_s = 200~425 kg/m^2·s), there is no net downflow of particles near the wall, and the cross-sectional average solids volumetric concentrations range from 0.1 to 0.20, with little axial variation in their relatively short riser (H = 6.1 m). The gas dispersion experimental results of Liu et al.[16] for the same system have shown that gas backmixing becomes small for high-density operating conditions where there is no downflow of solids near the riser wall. Based on these facts, Grace et al.[8] proposed a new flow regime termed as "dense suspension upflow (DSU)" to characterize the flow behaviors in the high-density CFB riser, and claimed that this flow regime can be archived when both superficial gas velocities and high-solids circulation rates are high (U_g > 5 m/s, and G_s > 200 kg/m^2·s). More recently, Bi[17] further investigated the gas and solids mixing in high-density CFB risers. His results showed that there exists a clear transition of both gas and solids axial mixing behavior when the operating conditions change from low-density to high-density operation, in correspondence to the disappearance of solids downward flow near the wall region. On the other hand, the experimental results of Issangya et al.[13–15] also showed that radial solids concentration profiles at high-solids circulation rates (G_s > 300 kg/m^2·s) are less uniform than those under lower solids circulation rates (G_s < 200 kg/m^2·s). Therefore, the nonuniform radial gas and solids distribution, disadvantage of low-density CFBs exists in HDCFBs as well.[8,14]

Taking all favorable and unfavorable characteristics of CFBs, TFBs and HDCFBs into consideration, Zhu and Zhu[18] proposed a novel circulating-turbulent fluidized bed (C-TFB), which operates in a special mode with low superficial gas velocities and high solids circulation rates, resulting in a highly dense suspension and uniform axial flow structure. Their C-TFB design and operation is developed especially to overcome those disadvantages encountered in CFB, TFB and HDCFB reactors, while integrating the advantages of them, such as the high solids concentration, excellent gas-solid contacting and mixing, as well as largely reduced axial solids back-mixing with high-solids circulation rates. The preliminary study of Zhu and Zhu[18] has shown that the high-density gas-solid suspension, having solids volume concentration of 20–30%, could be maintained throughout the entire C-TFB and that the C-TFB also exhibited an almost homogeneous axial flow structure with no net downflow of solids across the whole column cross section under all operating conditions.

Based on the preliminary study of Zhu and Zhu,[18] Zhu and Zhu[19] examined the differences of macro flow behaviors in the C-TFB, TFB, CFB and HDCFB. Their comparison has shown that the hydrodynamics in the C-TFB are different from those in the "regular" TFB, the conventional CFB and the high density CFB. However, a full understanding of the flow behaviors in C-TFBs is not complete until microflow structure is also studied. Then, it will be possible to delineate the flow regime in C-TFBs, in comparison with that in TFBs, CFBs and HDCFB. Therefore, this work focuses on the microhydrodynamic distinctions between the four fluidized beds. A novel multifunctional optical fiber probe was used to measure the instantaneous local solids concentration and particle velocity simultaneously in a "regular" turbulent fluidized, a circulating-turbulent fluidized bed riser, a conventional circulating fluidized-bed riser and a high-density circulating fluidized-bed riser.

Experimental Apparatus

All experiments were conducted in a combined fluidized bed system, schematically shown in Figure 1. The system includes two fluidized beds, the righthand fluidized bed

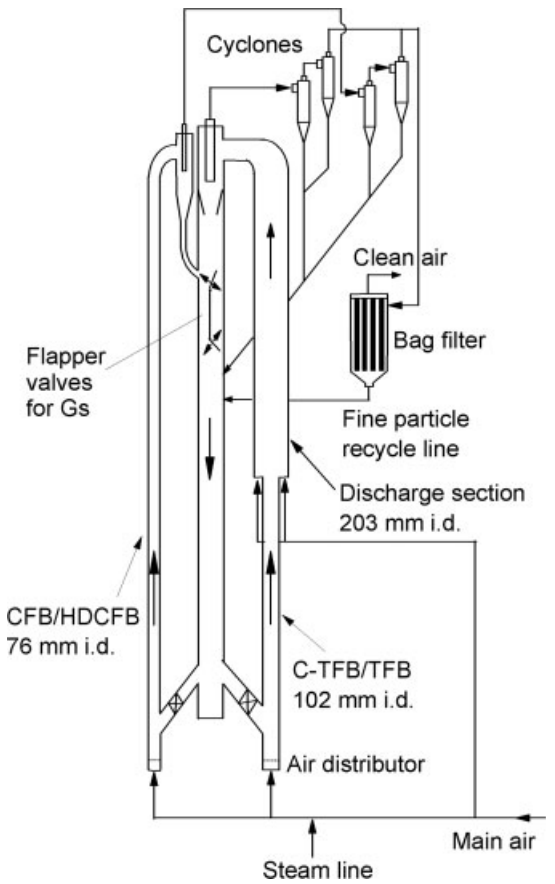

Figure 1. Schematic drawing of C-TFB, TFB, CFB and HDCFB systems.

serves as the newly proposed circulating-turbulent fluidized bed and a conventional turbulent fluidized bed, and the left-hand fluidized bed serves as a conventional circulating fluidized bed and a high-density circulating fluidized bed. A common downcomer with an inner diameter of 0.305 m and a height of 8.0 m was used for solids storage and return for both fluidized beds. Total solids inventory in the downcomer was about 420 kg, equivalent to a height of approximately 6.0 m. This high solids level ensures a high-pressure head in the downcomer, and enables high solids circulation rates and high-suspension density in both fluidized beds on the two sides. The column shown on the right consists of two sections: a C-TFB column at the bottom, with i.d. of 0.1 m and a 3.6 m height; and a discharging section above the C-TFB column with a diameter of 0.2 m, and a total height of 6.4 m for quick solids discharging. Secondary air supply was added into the upper discharging section via an annular perforated plate with 12.6% free area at the bottom of the discharging column to lift the particles upwards and to entrain particles out of the discharging column as quickly as possible, so that the pressure drop in the discharging section was minimized. Our preliminary studies had shown that the secondary air flow velocity in the upper discharging section would influence the operation in the lower C-TFB column, when a dense phase section begins to appear at the bottom of the discharging section. To minimize the effects of the secondary air supply on the hydrodynamics in the C-TFB, the secondary airflow velocity in the discharging section was kept at 5.0 m/s, under which there was no visible dense phase section at the bottom of the discharging section. The airflow rates were independently controlled in each section to allow the flexible operation over a wide range of gas velocities and solids circulation rates. For the operation in the conventional TFB, the static bed height was kept at 1.8 m. The conventional CFB and high-density CFB operation were conducted in the column on the left, with an inner diameter of 0.076 m, and a height of 10 m. More details about the fluidized-bed system can be found in Zhu and Zhu.[19]

In order to minimize the electrostatics found in the two columns, the whole fluidized-bed system was electrically grounded. At the same time, a small stream of steam was introduced into the main air pipeline to humidify the fluidization air to a relative humidity of 50–60%. This has been shown to be very effective to control the electrostatic effects.[20]

The fluidization gas used in this study was air at ambient temperature and pressure, supplied by a Roots-type blower. Particles used in this work were FCC catalysts (Sauter mean diameter d_p = 65 μm, particle density ρ_p=1,780 kg/m^3). A series of orifice plates were employed to measure the gas-flow rates. A solids circulation rate measuring device is located at the top of the downcomer sectioning the column into two halves with a central vertical plate, and two half butterfly valves fixed at the top and the bottom of the two-half section. By appropriately flipping over the two valves from one side to the other, solids circulated through the system can be accumulated on one side of the measuring section for a given time period, and then the solids circulation rate can be obtained.

Due to the requirement for in-depth investigation of dynamic transient flow behaviors in these gas-solid flow systems, much attention has been paid to the measurement device for the instantaneous local solids concentration, particle velocity and corresponding solids flux, which are indispensable to characterize the microtransient hydrodynamics in fluidized-bed reactors. Reflective-type optical fiber probes were widely used to measure the local solids concentrations and particle velocities in fluidized-bed reactors due to their simplicity, high accuracy, quick response and relatively low cost.[21–25] They yield high signal-to-noise ratios and, if properly designed, their small size does not significantly disturb the overall flow structure in fluidized beds.[22,26,27] More importantly, they are nearly free of interference by temperature, humidity, electrostatics and electromagnetic fields.[26,27,28] The optical fiber probes used in our experiments are model PV-5, newly developed by the Institute of Process Engineering, Chinese Academy of Sciences, Beijing, China. The probe and measurement procedure are schematically shown in Figure 2. The outer diameter of the probes is 3.8 mm, containing two subprobes. Each of the two subprobes consists of a boundless of quartz fibers arranged in square shape, and the effective distance of the two subprobes is 1.7 mm, and the active tip area of each subprobe is 1 $\times$ 1 mm. Each subprobe consists of many quartz fibers, both light-emitting and receiving, arranged in an alternating array, each 25 μm in diameter.

As shown in Figure 2, the received light reflected by the particles is multiplied by a photomultiplier and converted into voltage signals. The voltage signals are further amplified and fed into a PC. In principle, when moving particles pass the tips of the two subprobes, they would produce two similar signals only with a time shift T_{AB}, which can be calculated by cross-correlation method. Combining the time shift T_{AB}, with the effective distance between the two subprobes L_e, instantaneous particle velocity can be obtained. For the calculation of the particle velocities, an integration time T_d of 10.24 ms was set, after an optimization. In fluidized beds, the particle velocity calculated within such a short time period as 10.24 ms can be considered as transient velocity. Because of the turbulence of gas-solid suspension in fluidized beds, a particle passing through the upstream subprobe tip may not be detected by the downstream subprobe, due to the collisions or friction between the particles and the probe. This may lead to cross-correlation coefficients to be low or even indeterminate. Such poorly or uncorrelated data need to be eliminated. In this study, in order for the results to be acceptable, the correlation coefficients were required to be greater than 0.6 and the calculated velocities were required to differ by no more than five standard deviations from the average value.[23,28] The direction of the particle movement was determined based on the maximum cross-correlation coefficient from the positive and negative correlation of the two channel signals, yielded by the two subprobes.

On the other hand, the voltage data, in proportion to the reflective light intensity by the particles in the fluidized beds, can be converted to solids concentration by a predetermined calibration equation. Since the measuring volume of the optical fiber probes varies with the solids-volume concentration in fluidized beds, introducing error into the measurement by this technique, proper calibration is essential for this technique. A reliable and precise calibration, described in detail by Zhang et al.[26] was carried out to ensure accurate measurements.

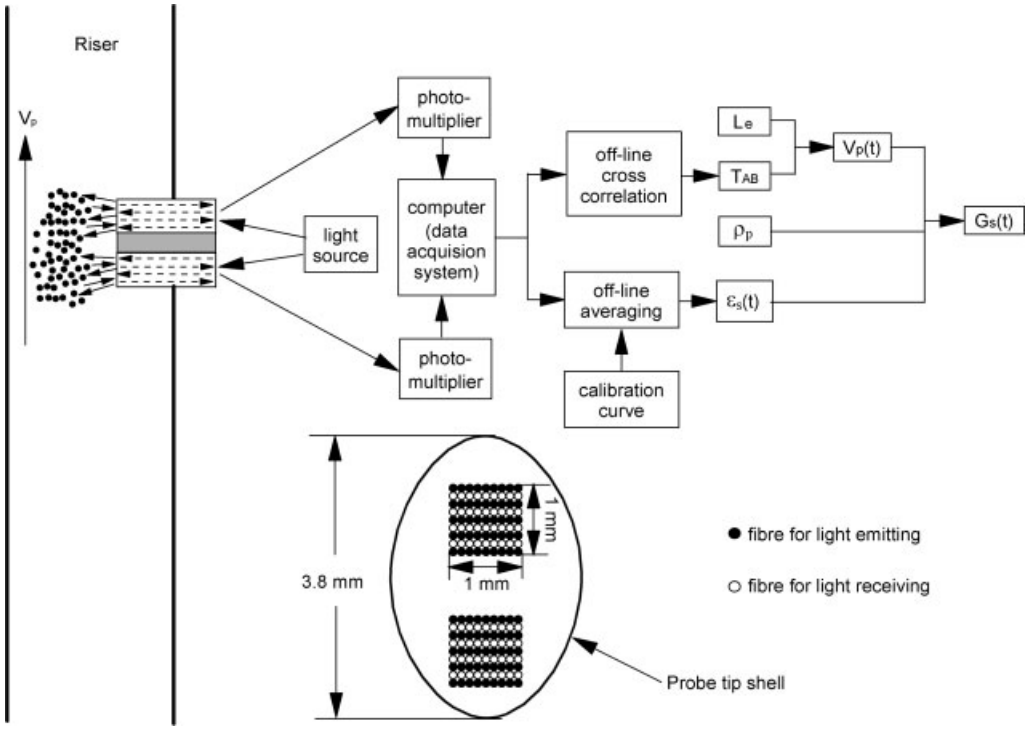

Figure 2. Schematic of the solids concentration-velocity fiber optic probe.

Since the multifunctional optical fiber probe is capable of measuring instantaneous local solids concentration and particle velocity simultaneously, the instantaneous local solids flux, can, thus, be calculated as

$$G_s(t) = \rho_p \bar{\varepsilon}_s(t) V_p(t) \tag{1}$$

where $V_p(t)$ is the instantaneous particle velocity, and $\bar{\varepsilon}_s(t)$ is instantaneous time-averaged solids concentration within the integration time period, T_d (=10.24 ms)

$$\bar{\varepsilon}_s(t) = \frac{1}{T_d} \int_0^{T_d} \varepsilon_s(t) \mathrm{d}t \tag{2}$$

By comparing the overall solids circulation rate G_s, measured by the flapper valves in the measuring tank, with the cross-sectional average solids flux G_s^*, integrated local time-mean solids fluxes across the riser crosssection, Zhu and Zhu[18] validated the measurement accuracy of the probe, indirectly verifying the reliability of both particle velocity and solids-volume concentration measured by the probe.

Local solids concentration and particle velocity were measured at 11 radial positions (r/R = 0.00, 0.16, 0.38, 0.50, 0.59, 0.67, 0.74, 0.81, 0.87, 0.92 and 0.98) on two axial levels (z = 0.8 and 1.5 m) of all four kinds of fluidized beds (C-TFB, TFB, and the bottom region of CFB and HDCFB). To map the full spectra of particle velocity and solids concentration signals, 163,840 data points were sampled with a sampling frequency of 50 kHz at each measuring location. To ensure the validity and repeatability, all measurements are repeated at least five times. It should be noted that experiments on the C-TFB have been carried out under a wide range of operating conditions, but only results from two typical operating conditions in the C-TFB are presented here for comparison with TFB and the bottom region of CFB and HDCFB. For more results, please refer to Zhu and Zhu[18] and our publication in the near future.

Results and Discussion

Instantaneous solids concentration

Local instantaneous solids concentration and its fluctuations reflect the transient behavior of the interaction between the gas and solid phases, and then influence the gas-solid contacting efficiency and heat/mass transfer properties in fluidized beds.[29] To compare the turbulence of local gas-solid suspension flow in C-TFBs, TFBs and the bottom region of HDCFBs, Figure 3 plots local solids concentration traces obtained by the multifunctional optical fiber probe at four radial positions on the same axial level under typical conventional turbulent, circulating-turbulent and high-density circulating fluidization conditions, respectively. Clearly, the solids concentrations at most radial positions in the HDCFB are much lower that those in the TFB and C-TFB, while the solids concentrations in the TFB and C-TFB are nearly the same. This suggests that the gas-solid flow dynamics in the HDCFB are quite distinct from those in the C-TFB and TFB. In the HDCFB, as shown in Figure 3, the most transient solids concentrations at most radial positions ($r/R < 0.98$) are of low value, indicating that dilute gas-solid suspension dominate at most space and time in the HDCFB. There are still some higher-solids concentration peaks, which reflect the formation of clusters. Moreover, the fluctuations of the solids concentration increase from the center to the wall. With increasing radial position, more and more relatively dense

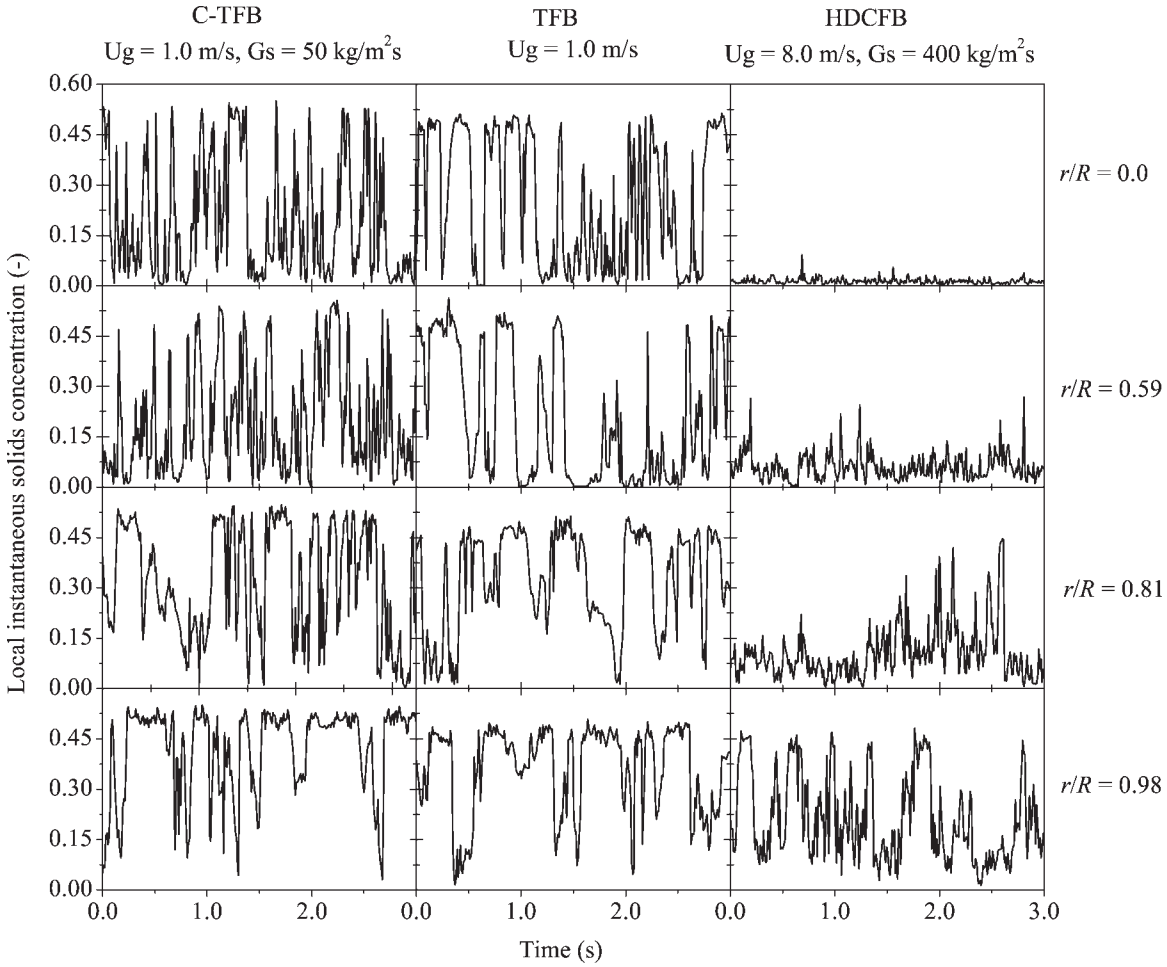

Figure 3. Comparison of solids concentration traces in the C-TFB, TFB and HDCFB at the same axial level (z = 0.8 m).

clusters are formed, and the solids fluctuation becomes more vigorous. The corresponding probability distribution analyses of the instantaneous solids concentrations in the HDCFB by Zhu and Zhu[18] have also shown that the gas-phase tends to pass mostly through the core region, while the particles are more visible in the wall region.

Comparing the solids concentration traces in the C-TFB and TFB (shown in Figure 3), one can find that although the time series of instantaneous solids concentration in the C-TFB and TFB are somewhat similar, there are also some noticeable differences. In the central region of the column for both TFB and C-TFB, the solids concentration is high and accompanied by high-amplitude fluctuations, different from the characteristics of the solids concentration trace in the same region of the HDCFB. Moving outward toward the column wall, the frequency of higher-solids concentrations decreased as the suspension becomes denser, leading to a more continuous solids concentration distribution. Close to the wall, the fluctuations start to die down, with the low-solids concentration peaks becoming less frequent and the flow is predominated by dense phase. A low-solids concentration probability peak is no longer observed, being replaced by a high-concentration peak.[18] However, the transient solids-concentration and its fluctuations as shown in Figure 3 demonstrate that the solids-concentration distributions in the C-TFB are much more continuous than that in the TFB. In other words, compared with the flow structure in the C-TFB, a much more clear-cut two phase structure in the conventional TFB can be observed. One phase could be termed as void/dilute phase with low-solids concentration; the other phase as dense/cluster phase with high-solids concentration. On the other hand, due to intenser turbulence and more frequent fluctuations of local solids concentrations in the C-TFB than those in the TFB, the distinction between the void/dilute and dense/cluster phase in the C-TFB is more diffuse even lost completely. The solids concentration in the dense-phase in the C-TFB is lower compared to the case of the TFB. It is also observed from Figure 3 that the dense phase gradually disperses into a gas-phase, and finally becomes a somewhat dispersed phase. This continuous distribution of transient solids concentration indicates that the dense-phase in the C-TFB contains more gas than in the TFB, and more particles entered the void/dilute phase, resulting in stronger particle-particle collisions and more vigorous fluctuations of gas-solid suspension occurring at higher-frequency. With increasing particle-particle interactions (collisions), the segregation of the gas-phase from the solids-phase is gradually suppressed and a more homogenous flow pattern results.[30] The vigorous fluctuations and strong turbulence result in better gas/solids contacting quality, and, thus, reduced gas by-passing, which

occurs in the core region of the HDCFB risers. This excellent contacting and mixing characteristic, vigorous particle-particle interactions and interpenetration between the gas-and solid-phases, at almost all radial positions is a great advantage of C-TFBs over TFBs and HDCFBs.

To further compare the transient dynamic behaviors of the gas-solid flow in the C-TFB and TFB, another parameter is used to characterize instantaneous solids concentration time-series signals, cycle frequency, defined as the number of times per second that an instantaneous solids concentration crosses its time-averaged value. Higher cycle frequencies correspond to higher Kolmogorov entropies, and, thus, to more complex dynamic gas-solid flow system in the fluidized beds.[31] Figure 4 shows the cycle frequencies in term of solids concentration in the C-TFB and TFB. In the near wall region ($r/R > 0.81$), the cycle frequencies in the C-TFB and TFB are very close, suggesting there is no marked difference between the turbulence intensity of gas-solid suspension (also see Figure 3). The cycle frequencies in the TFB change little with the radial position. However, the cycle frequencies in the C-TFB are seen to be a strong function of the radial position, with a maximum value of about 225 Hz at the column center, and decreasing to about 50 Hz at the wall, indicating that the closer to the column center, the intenser the turbulence of gas-solid suspension. This suggests that the dynamic behaviors of the gas-solid suspension in the center region of the C-TFB are quite different from those in same region of the TFB.

Figure 5 compares the instantaneous local solids concentrations in the CFB and C-TFB under the same operating condition. Clearly, an evident distinction can be observed between the C-TFB and TFB although the operating condition is the same. From Figure 5, it can be seen that dilute gas-solid suspension dominates most space of the CFB column at most time. Moving from the center toward the wall, although the suspension becomes denser, only a single peak was observed in the profiles of solids concentration probability density distribution.[18] From the results, it is clear that in the bottom region of CFB, the gas-phase tends to pass mostly through the core region, while the solids most concentrate in the wall region. Due to the separation of the gas-phase from the solids-phase, the gas-solid contacting and mixing becomes less ideal in conventional circulating fluidized beds.[32] However, for the case of circulating turbulent fluidization system, the broad and continuous spectrum of transient solids concentration in the C-TFB suggests that the gas and solid phases have a greatly improved mixing, and the dense pockets have a continuous variation in solids concentration. This is a key advantage of C-TFBs over CFBs.

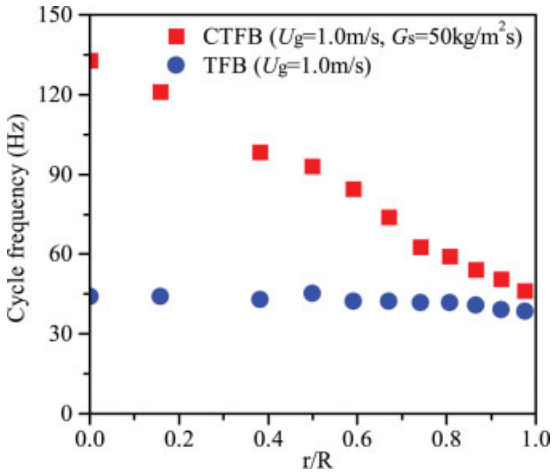

Figure 4. Radial profiles of cycle frequency in the C-TFB and TFB on the same axial level (z = 0.8 m).

[Color figure can be viewed in the online issue, which is available at www.interscience.wiley.com.]

The probability density distribution (PDD) of the instantaneous local solids concentration is a great help in understanding the interaction between the gas and solids phase. Zhu and Zhu[18] compared the probability density distributions of solids concentration in various radial positions of the TFB, CTFB and HDCFB. Their results showed that the single-peak PDDs in the HDCFB indicated that the flow behavior was mainly controlled by dilute phase corresponding to the relatively low fluctuations in the solids concentration. The broad and continuous spectrum of solids concentration in the TFB and C-TFB indicated that the dense-phase contained more gas than the HDCFB, and more particles entered the void/dilute phase, and the clusters have a continuous variation in solids concentration.[19] As a result, the aforementioned differences in the transient behavior of gas-solid suspension suggest that different mechanisms dominate the interactions between the gas and solid phases in the three fluidization systems. At the same time, it can also be concluded that time-averaged parameters are not sufficient to characterize the differences of transient dynamic behaviors of gas-solid suspension in the various fluidization regimes.

Time-mean solids concentration

Since the knowledge of axial and radial flow structures in fluidized beds is key to fully understanding, successful design and proper operation of these reactors, the local solids concentration distributions were investigated in both axial and radial directions of the CFB, TFB, CTFB and HDCFB.

Figure 6 compares the axial solids concentration distribution in the TFB, C-TFB, CFB and HDCFB against the dimensionless height h/H. Clearly, an extremely axial uniform solids concentration distribution in the C-TFB can be found in Figure 6, compared with the substantial variation in solids concentrations with a dense-phase at the bottom and a dilute region toward the top of the TFB, CFB and HDCFB. As shown in Figure 6, the axial solids distribution profile in the TFB and CFB was significantly nonuniform. At the bottom of the TFB, the solids concentrations are as high as 0.35 and thereafter decrease significantly with height, finally reaching 0.02 at the top section. In the CFB, an axial nonhomogeneity was also observed, with the solids concentrations decreasing from 0.2 at the bottom to 0.05 at the top. Compared with axial flow structure in the TFB and CFB, the axial uniformity of solids concentration distribution in the HDCFB is improved in some degree, but it is still more nonuniform than that in the C-TFB.

In the C-TFB, a high-density and uniform axial gas-solid suspension distribution has been achieved along the whole column, with solids concentrations ranging from 0.25 to 0.3.

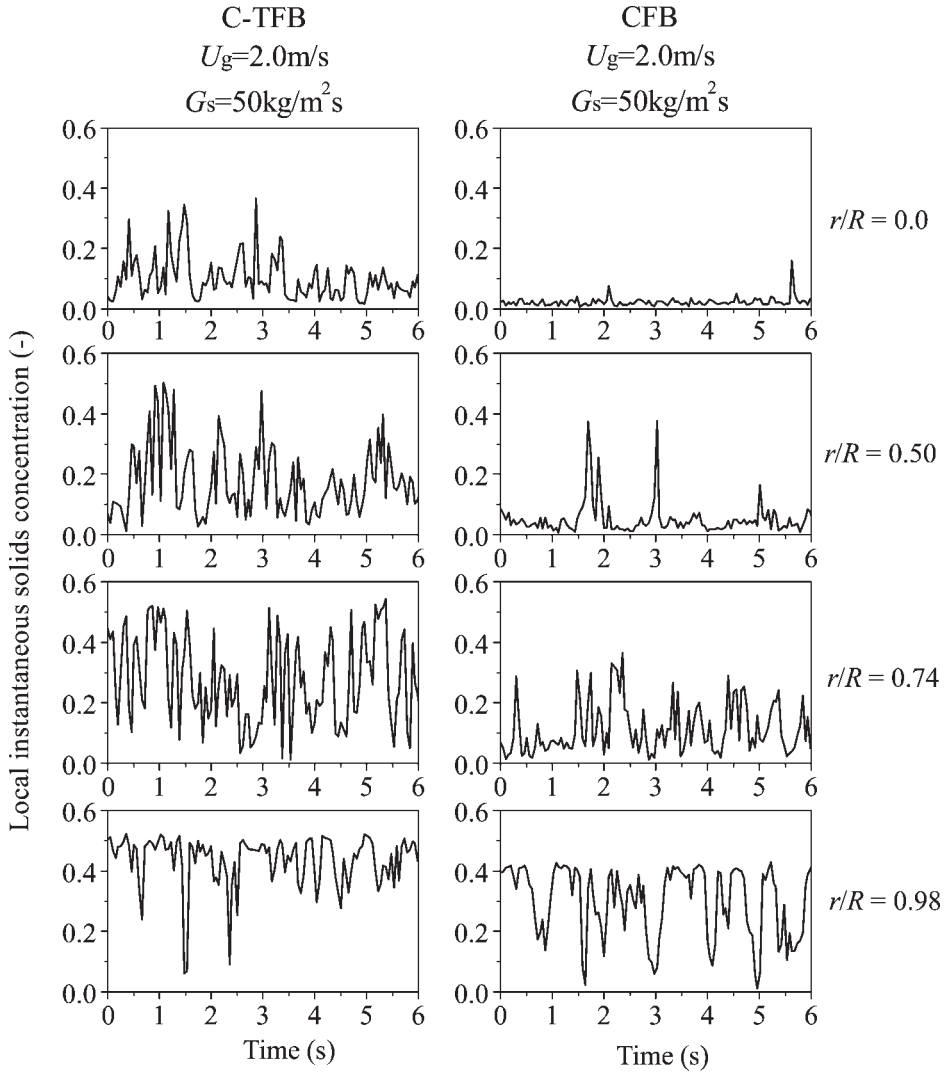

Figure 5. Comparison of instantaneous solids concentration in the C-TFB and CFB at the same operating condition and axial level (z = 1.5 m).

Such solids concentrations in the C-TFB are slightly lower than those in the bottom region of the TFB (~0.35), but higher than those in the bottom dense region of the CFB (~ 0.2), and those in the HDCFB (0.15 ~ 0.25), as shown in Figure 6. The axial uniform flow structure in the C-TFB should lead to both uniform gas-solid contact efficiency and uniform suspension-to-wall heat transfer throughout the entire C-TFB.

Typical radial profiles of time-mean solids concentration on the same axial level of the C-TFB, TFB, HDCFB and CFB are presented in Figures 7a and 8a. In all fluidized beds, the time-mean solids concentrations all increase monotonically from the column center to the wall, but the radial solids concentration distribution in the C-TFB and TFB are much more uniform than that in the HDCFB and CFB. Obviously, the solids concentration and its radial distribution in the C-TFB are closer to those of the conventional TFB, more different from those sharply demarcated "core-annulus" flow structure with dilute core region, and dense annulus region in the CFB and HDCFB. The standard deviation of solids concentration in the CFB and HDCFB also confirmed that a clear-cut "core-annulus" structure with a dilute and homogenous core region surrounded by a dense and fluctuating annulus zone still existed in the CFB and HDCFB, even when the corresponding cross-sectional average solids concentration was as high as 0.21.[19] With electrical capacitance tomography, Malcus et al.[33] also found that a "core-annulus" flow structure in the high density bottom zone of the CFB riser and that within the bottom zone the flow structure vary little with a change in height or external solids mass flux. Since high-solids volume concentration significantly increases interactions between gas and particles, the contacting efficiencies between gas and particles in the center region of the C-TFB, may be much higher than those in the CFB and HDCFB, leading to much higher heat/mass transfer rate in the center region of the C-TFB, and then more uniform radial distribution of contacting efficiency. At the same time, the high solids concentration in the C-TFB would also results in a higher effective viscosity of gas-solid suspension,[8] thereby, imposing more shear on the descending particles and

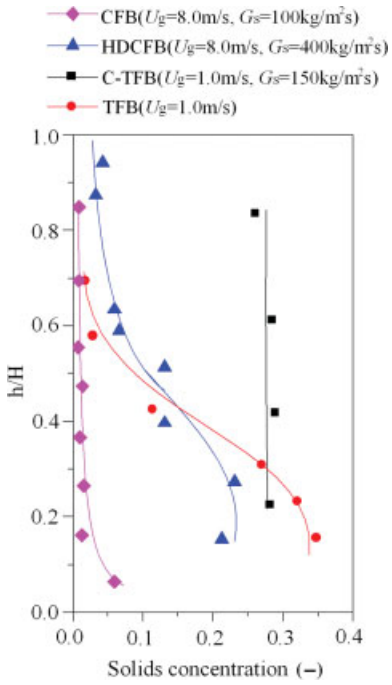

Figure 6. Axial profiles of solids concentration distribution in the TFB, C-TFB, CFB and HDCFB.

[Color figure can be viewed in the online issue, which is available at www.interscience.wiley.com.]

reducing the tendency for the solids downflow. As a result, there is no net solids back-mixing in the C-TFB,[18] leading to a reduction in axial dispersion of both gas and solids.

Zhu and Zhu[18] presented the solids concentration measurements from two different radial directions with an angle of 120° apart on the same axial level. Their results showed that under all operating conditions in their study, there was little difference between the solid concentrations obtained from the two radial directions. Therefore, the cross-sectional distribution of time-averaged local solids concentrations in the C-TFB may be considered as an axisymmetrical distribution, even at the bottom region, where the flow structure was prone to be affected by the gas distributor structure or solids inlet type.

Intermittency index

Segregations of the gas-phase from the solid-phase can be reflected quantitatively by the intermittency index of gas-solid flow in terms of the local solids concentration, which would be zero for perfect core-annulus flow and one for perfect cluster flow.[34] To compare the extent of the segregation between the gas and solid phases in the different flow regimes, radial profiles of intermittency index on the similar axial levels of the C-TFB, TFB, CFB and HDCFB are plotted in Figures 7b and 8b. The comparison of the intermittency index profiles in the C-TFB, TFB, CFB and HDCFB shows some similarity. In general, all the radial profiles of intermittency index increase with radial position, to a maximum at an intermediate radial position around r/R = 0.6~0.8 and decrease thereafter toward the wall. A possible explanation could be that lower-solids concentration in the center region and higher-solids concentration in near wall region induce less fluctuations and turbulence (as shown in Figures 15 and 16), and then result in greater phase segregation. Despite the aforementioned similarities, quite a difference happens in the intermittency index profiles between the C-TFB, TFB, CFB and HDCFB. First, the intermittency indexes in the C-TFB and TFB are much higher than those in the CFB and HDCFB across the whole column cross section, indicating that the extents of the segregation of the gas-phase from the solids-phase in the CFB and HDCFB are much greater than those in the C-TFB and TFB. Second, compared with C-TFB and TFB, the intermittency indexes in the core region of the CFB and HDCFB are much lower, and, thus, the radial profiles of intermittency index in the CFB and HDCFB are less uniform than those in the C-TFB and TFB. The extremely nonuniform distribution of intermittency index in the CFB and HDCFB may be due to the significant gradient in radial distribution of local gas velocity, as high as 10 m/s in the center, and as low as 0.6 m/s at the

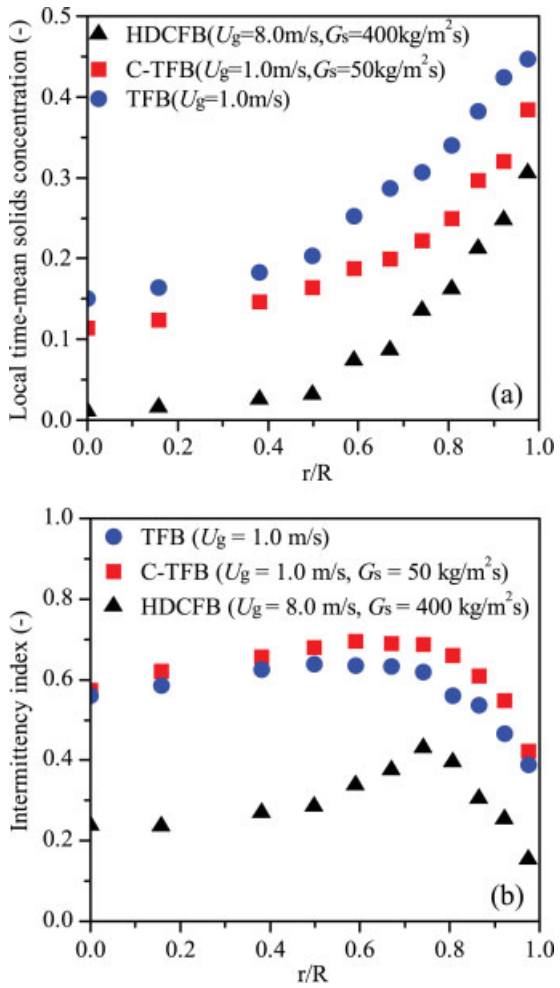

Figure 7. Radial profiles of (a) time-mean solids concentration, and (b) intermittency index in the C-TFB, TFB and HDCFB at the same axial level (z = 0.8 m).

[Color figure can be viewed in the online issue, which is available at www.interscience.wiley.com.]

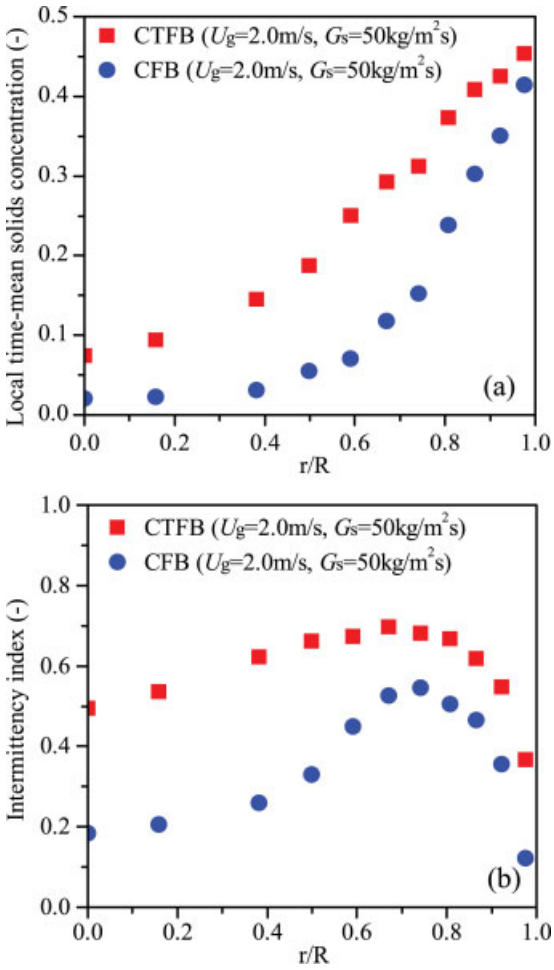

Figure 8. Radial profiles of (a) time-mean solids concentration, and (b) intermittency index in the C-TFB and CFB at the same operating condition and axial level (z = 1.5 m).

[Color figure can be viewed in the online issue, which is available at www.interscience.wiley.com.]

wall, coupled with dilute solids concentration in the core region and much denser solids concentration in the wall region. This serious radial separation of the gas-phase from the solids-phase in the CFB and HDCFB would result in reduced gas-solid contacting and mixing.[32] However, for the dense conditions, such as in the C-TFB and TFB, the relative low superficial gas velocities lead to a more uniform distribution of local gas velocity across the column section, and, therefore, a more uniform solids concentration, particle velocity and solids flux.[18] This better hydrodynamic characteristic in the C-TFB would consequently, improve reactor performance, such as more uniform gas and solids contact efficiency in radial direction and residence-time distribution of gas and solid phases. Furthermore, it can also be noted from Figure 7b that the intermittency index and its radial profiles in the C-TFB and TFB are almost the same, suggesting an inherent similarity in the gas-solid flow between these two types of fluidized bed.

Time-mean particle velocity

Particle velocities are very important in affecting gas-solid contacting and mixing, heat/mass transfers as well as erosion in fluidized beds. Particle velocity distribution is also directly related to the residence time of particles within fluidized-bed reactors. Figures 9 and 10 display the radial profiles of local time-mean particle velocity in the C-TFB, TFB, CFB and HDCFB, respectively. In general, the maximum particle velocity occurs at the column axis, and it decreases monotonically with the radial position moving outward toward the bed wall. In spite of the aforementioned similarity, obvious difference can be seen between the particle velocity profiles in the C-TFB, TFB, CFB and HDCFB. Compared with the radial distributions of particle velocities in the C-TFB and TFB, the radial particle velocity profiles in the HDCFB are extremely nonuniform, as high as 10.6 m/s in the center and as low as 0.6 m/s at the wall, as shown in Figure 9. This radial nonuniformity of particle velocity distribution may be caused by the high superficial gas velocity, that is, the high superficial gas velocity leads to significant difference between the local gas velocity at the center and the one at the wall, coupling with the help of gravity, which results in remarkable segregation of the solids from the core region to the wall region. Obviously, this significant radial nonuniformity of particle velocity and/or gas velocity in the HDCFB definitely results in a wide residence-time distribution of particles and/or gas, unfavorable for chemical reactions in which high selectivities are crucial. Close to the wall, although the difference of particle velocities in the C-TFB, TFB, CFB and HDCFB becomes smaller, the time-mean particle velocities near the wall of the C-TFB and HDCFB are still above zero and the particles in the wall region of the TFB mainly flow downward. On the other

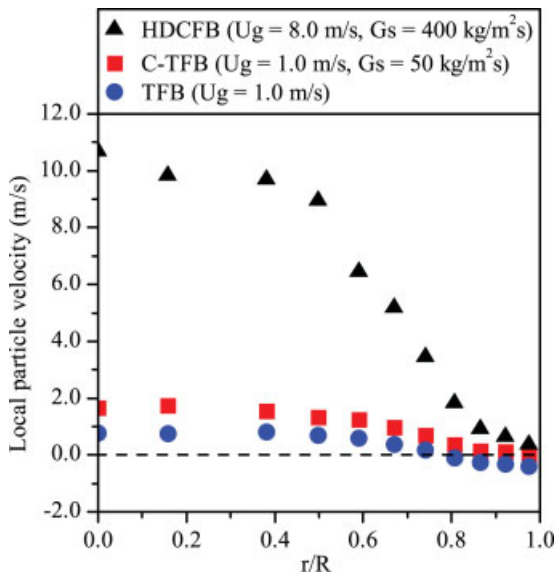

Figure 9. Radial profiles of time-mean particle velocity: in the C-TFB, TFB and HDCFB at the same axial level (z = 1.5 m).

[Color figure can be viewed in the online issue, which is available at www.interscience.wiley.com.]

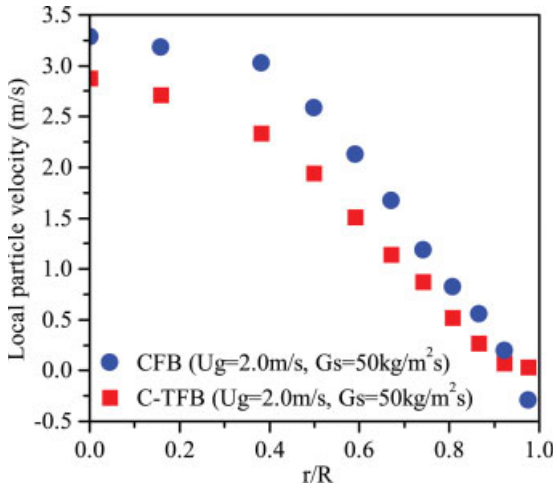

Figure 10. Radial profiles of time-mean particle velocity in the C-TFB and CFB at the same operating condition and axial level (z = 1.5 m).

[Color figure can be viewed in the online issue, which is available at www.interscience.wiley.com.]

hand, as shown in Figure 10, the particle velocities in the C-TFB are slightly lower than those in the conventional CFB under the same operating condition except at the radial position near the wall. This is expected since in most area of the cross section except the radial positions near the wall, the solids concentrations in the C-TFB are much higher than those in the same radial positions of the conventional CFB under the same cross-sectional average solids flux (see Figure 8a). Close to the wall, the time-mean particle velocity in the C-TFB is positive, but the particles near the wall of the CFB mainly flow downward, as also shown more clearly in Figure 10. The reason for this difference may be also the higher-solids concentrations in the C-TFB than in the conventional CFB. A higher effective viscosity of the rising suspension, resulting from the higher solids concentrations in the C-TFB, would impose more shear stress on the descending particles.[8] At the same time, the higher-solids concentration would also provide more upward momentum to reduce the tendency for the descending particles by particle-particle interactions (collisions). No net downflowing solids flux near the wall is another key advantage of the C-TFB over the conventional TFB and CFB, leading to a reduction in axial dispersion of gas carried by the downflowing particles.

Relationship between instantaneous solids concentration and particle velocity

Local time-mean particle velocity and solids concentration in fluidized beds were found to be closely related to each other by Parssinen and Zhu[35] and Yan and Zhu.[36] However, in their studies, since their local time-mean solids concentration and particle velocity were measured by different probes at different time, the results cannot accurately reflect the transient relationship between local instantaneous solids concentration and particle velocity. Simultaneous measurements of instantaneous local solids concentrations and particle velocities can provide more detailed transient dynamic information on gas-solid suspension flow in fluidized beds. Simultaneous measurement of instantaneous local particle concentration and velocity can also help to determine the Reynolds stress components of particles motion.[37] Liu et al.[24] measured the local instantaneous particle velocities and solids concentrations in a high-density circulating fluidized-bed riser simultaneously with a multifunctional optical fiber probe. Their results have shown that at the center and the wall of the high-density circulating fluidized-bed riser, the local instantaneous particle velocities and the corresponding solids concentrations appear to be uncorrelated, while at the other radial positions, the local instantaneous particle velocities and the corresponding solids concentrations have a strong correlation, with highersolids concentration usually corresponding to lower particle velocities and dilute suspension mostly corresponding to higher upflow velocity. However, their probe is a single-fiber probe, not a multifiber probe, which cannot very precisely measure the local instantaneous solids volume concentration, especially for the particle clouds in the high-density circulating fluidized bed riser.

To investigate the relationship between the local instantaneous solids concentrations and particle velocities of particle clouds in the C-TFB, TFB and HDCFB, Figure 11 compares the instantaneous particle velocities against the instantaneous solids concentrations determined simultaneously by our novel multifunctional optical probe at three typical radial positions on the same axial level. Clearly, a strong correlation can be observed at most radial positions except for the one nearest the wall for the gas-solid flow in the HDCFB, with higher-solids concentrations corresponding to lower and even negative velocities, while dilute gas-solid suspension mostly corresponding to higher upflow particle velocities. Such a strong dependence suggests that the particle movements are mainly controlled by gas-particle interaction in the HDCFB, where the particle-particle interactions (collisions) are relatively weaker than the gas-particle interactions.[30,38] However, for the gas-solid suspension flow in the C-TFB and TFB, the instantaneous particle velocities and the corresponding solids concentrations appear to be uncorrelated at all radial positions. As shown in Figure 11, both solids concentrations and particle velocities all have a very wide distribution in the C-TFB and TFB. Under a wide range of solids concentrations, the particle velocities all vary from negative to positive values, indicating a random flow structure with intense fluctuations of solids concentrations and particle velocities in the C-TFB and TFB. Even for a very dilute gas-solid suspension flow in the C-TFB and TFB, the particles still have a wide distribution of velocities. This suggests that in the dense conditions, such as in the C-TFB and TFB, particles motion is mainly controlled by the particle-particle interactions (collisions), while the gas-particle interactions have less influence on the particle movements, since the local gas velocities in the C-TFB and TFB are much lower than those in the HDCFB and conventional CFB, resulting in much less drag forces exerted on particles by gas. This suggests that most portion of the particle momentum is transferred by interactions (collisions) between particles, but not by drag forces between gas and solid phases, like in HDCFB and conventional CFB. As a result, it could be concluded that circulating-turbulent fluidization flow regime and dense suspension upflow flow regime are essentially different.

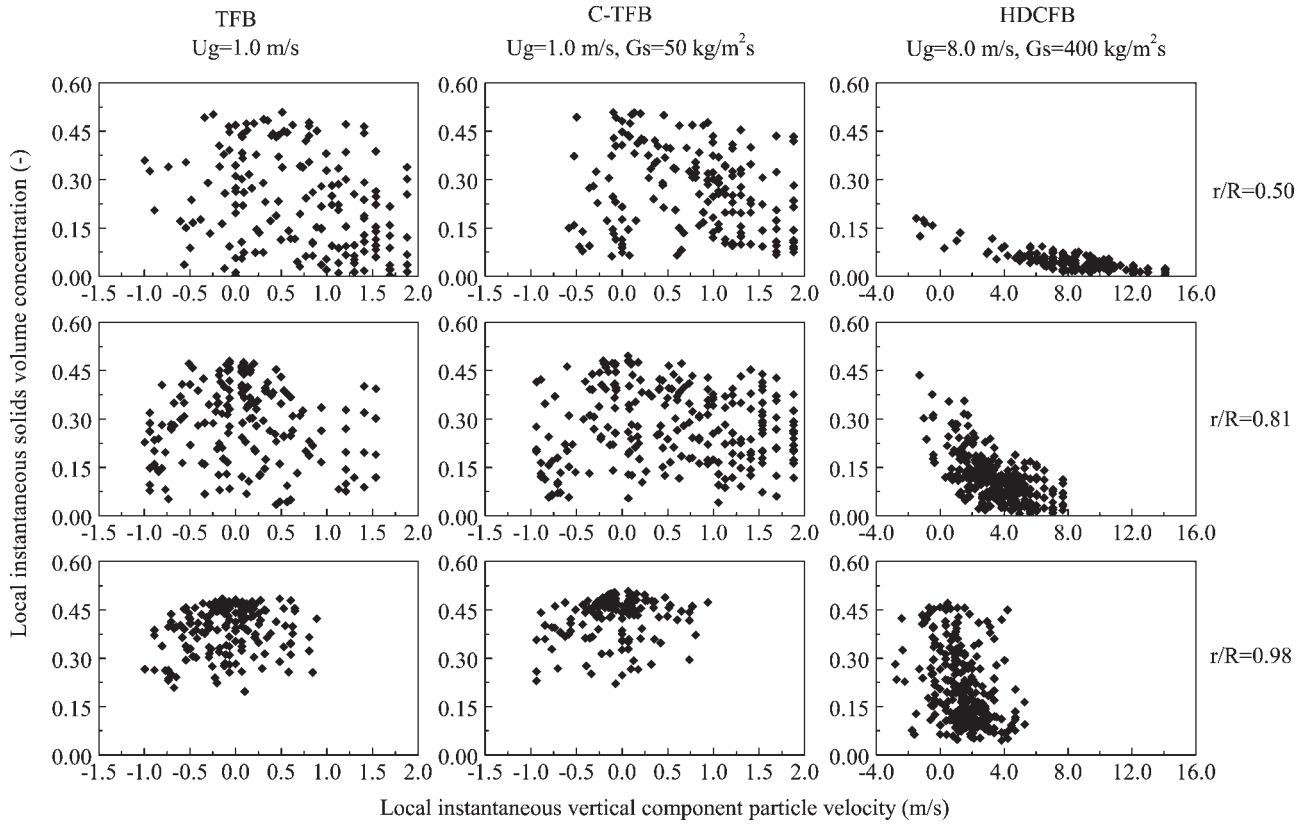

Figure 11. Local instantaneous vertical component of particle velocity vs. simultaneously measured local instantaneous solids concentration in the C-TFB, TFB and HDCFB at the same axial level (z = 0.8 m).

Figure 12 displays the instantaneous particle velocities against the instantaneous solids concentrations measured simultaneously at the same radial and axial position under the same operating condition in the C-TFB and CFB. Similarly, the particle movements in the conventional CFB are dominated by the gas-particle interactions, while for the gas-solid flow in the C-TFB, the particle-particle collisions predominate over the drag forces between the gas and solid phases across the whole bed section.

The same phenomena can also be observed at all radial positions on all axial levels except for the near wall region of the HDCFB and CFB. This exception may be due to the significant effects of the bed wall on the gas-solid suspension flow. As a result, it could be concluded that the movements of particles in the conventional CFB and the HDCFB are controlled by the gas-particle interactions (drag forces), while the particle-particle interactions (collisions) dominate the motion of particles in the C-TFB and TFB. This further suggests that the interaction characteristics between the gas and solid phase in the C-TFB are essentially close to those in the TFB in this respect, but totally different from those in the conventional CFB and the HDCFB.

Instantaneous solids flux

Fluctuations in local instantaneous solids flux directly reflect turbulence of local gas-solid suspension flow dynamics. Isokinetic or nonisokinetic suction probes have been widely used to measure local time-averaged vertical solids fluxes in CFBs by many researchers.[39–42] However, this method cannot provide instantaneous solids flux information, and it is not very accurate for highly turbulent gas-solid suspension flow. Furthermore, the instantaneous solids flux time series give more detailed dynamic transient information than time-averaged one. In addition, the small size of the optical fiber probe will not create as much disturbance to the gas-solid flow as the suction probe does. Our newly developed multifunctional optical fiber probe is capable of measuring instantaneous solids fluxes and their fluctuations. Figure 13 compares the transient signals of local solids flux at four typical radial positions (r/R= 0.0, 0.59, 0.87 and 0.98) at the level of 0.8m above the gas distributor under typical turbulent, circulating turbulent and high-density fast fluidization conditions. Generally, in the central region, the instantaneous solids fluxes are relatively high in time-mean magnitude and also fluctuate with low-frequency and amplitude. This is reasonable since in the central region, the lower-solids concentrations (see Figure 7(a)), coupled with higher local gas velocities, tend to lead to the lower local solids fluxes and less frequent and lower fluctuations, due to less frequent formation and breakup of clusters. Moving outward towards the wall, the instantaneous solids fluxes appear to decrease in time-mean magnitude but accompanied by more vigorous fluctuations with higher frequency and amplitude. The vigorous fluctuations are due to the higher local solids concentrations and lower local gas velocities than those in the central

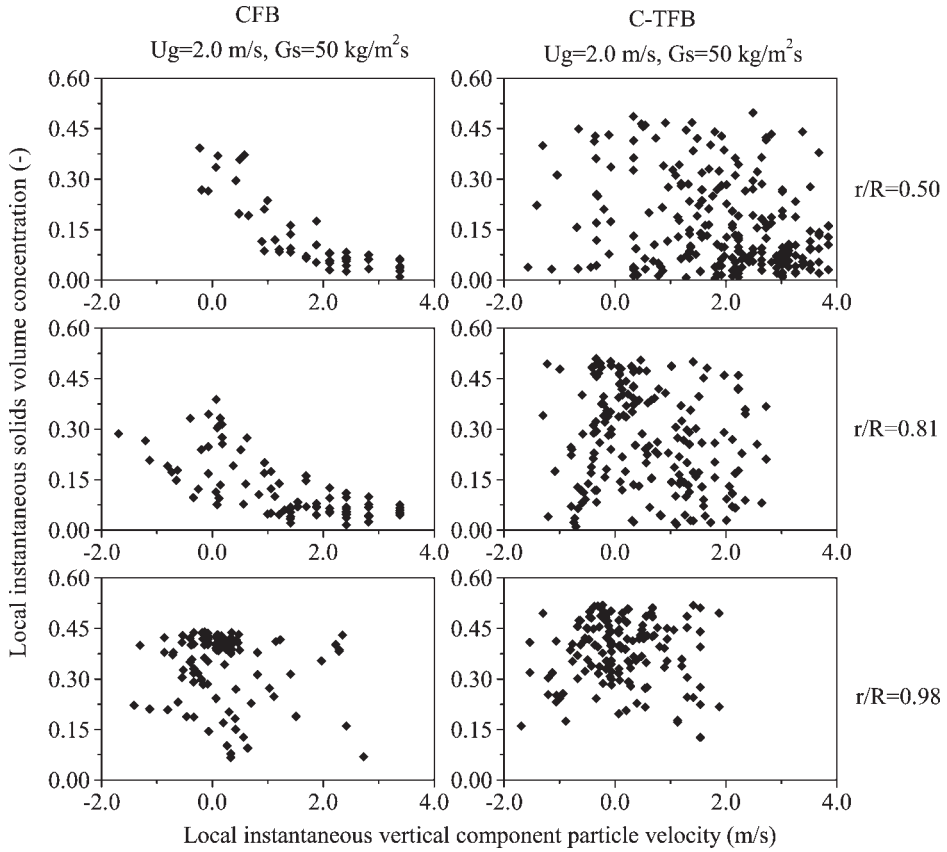

Figure 12. Local instantaneous vertical component of particle velocity vs. simultaneously measured local instantaneous solids concentration in the C-TFB and CFB at the same operating condition and axial level (z = 1.5 m).

region, resulting in more frequent formation and break-up of clusters, as well as stronger particle-particle collisions. Reviewing intensively the solids flux time series in the C-TFB, TFB and HDCFB plotted in Figure 13, noticeable differences can, however, be found among the three fluidized beds. Firstly, at the dilute center region (e.g., r/R = 0.0 and 0.59) of the HDCFB riser, most instantaneous solids fluxes are above zero, which means most particles are moving upward. However, in the same region of the C-TFB and TFB, quiet a few particles are moving downward. Second, in the intermediate region (e.g., r/R = 0.87), the instantaneous solids fluxes in the HDCFB fluctuate much more vigorous than those in the C-TFB and TFB (also see Figure 15). This is expected since the local gas velocities in this region of the HDCFB are higher than those in the same radial region of the C-TFB and CFB, but there are no big difference in the solids concentrations between the C-TFB, TFB and HDCFB (see Figure 7a), so that the traces of instantaneous solids flux in this region do not differ greatly. Also, as discussed above, the gas-solids interactions dominate the movements of gas-solid suspension across the whole HDCFB except at the wall, causing formation and break-up of clusters, while the motion of gas-solid suspension in the C-TFB and TFB is controlled by particle-particle interactions (collisions), whose collision frequencies are much higher than those of cluster formation and break-up. Consequently, the fluctuations amplitude of instantaneous solids fluxes in the intermediate region of the HDCFB is much higher than those in the same region of the C-TFB and CFB (also see Figure 15), but the fluctuations frequency of instantaneous solids fluxes in this region of the HDCFB is lower than those in the same region of the C-TFB and CFB, as shown in Figure 13. Third, Figure 13 also shows that the instantaneous solids flux time series in the whole C-TFB have higher frequency and amplitude than those in the TFB. After averaging the instantaneous solids fluxes time series, Zhu and Zhu[19] found that solids backmixing phenomenon, which is obvious in both turbulent fluidized beds and conventional circulating fluidized beds, is hardly observed in C-TFBs. This may be due to higher overall net external solids circulation rate and intenser particle-particle interactions in the C-TFB than those in the TFB.

A comparison of instantaneous solids fluxes in the C-TFB and the conventional CFB at the same axial level under the same operating condition is presented in Figure 14. Although the superficial gas velocity and solids circulation rate are the same in the two types of fluidized beds, the fluctuations frequency and amplitude and the time-mean value of the instantaneous solids flux time series in the C-TFB are quiet different from those in the conventional CFB. This difference can be attributed to the different interaction mechanisms between the gas and solid phases in the two types of flow regimes. As stated earlier, the particle-particle interactions (collisions)

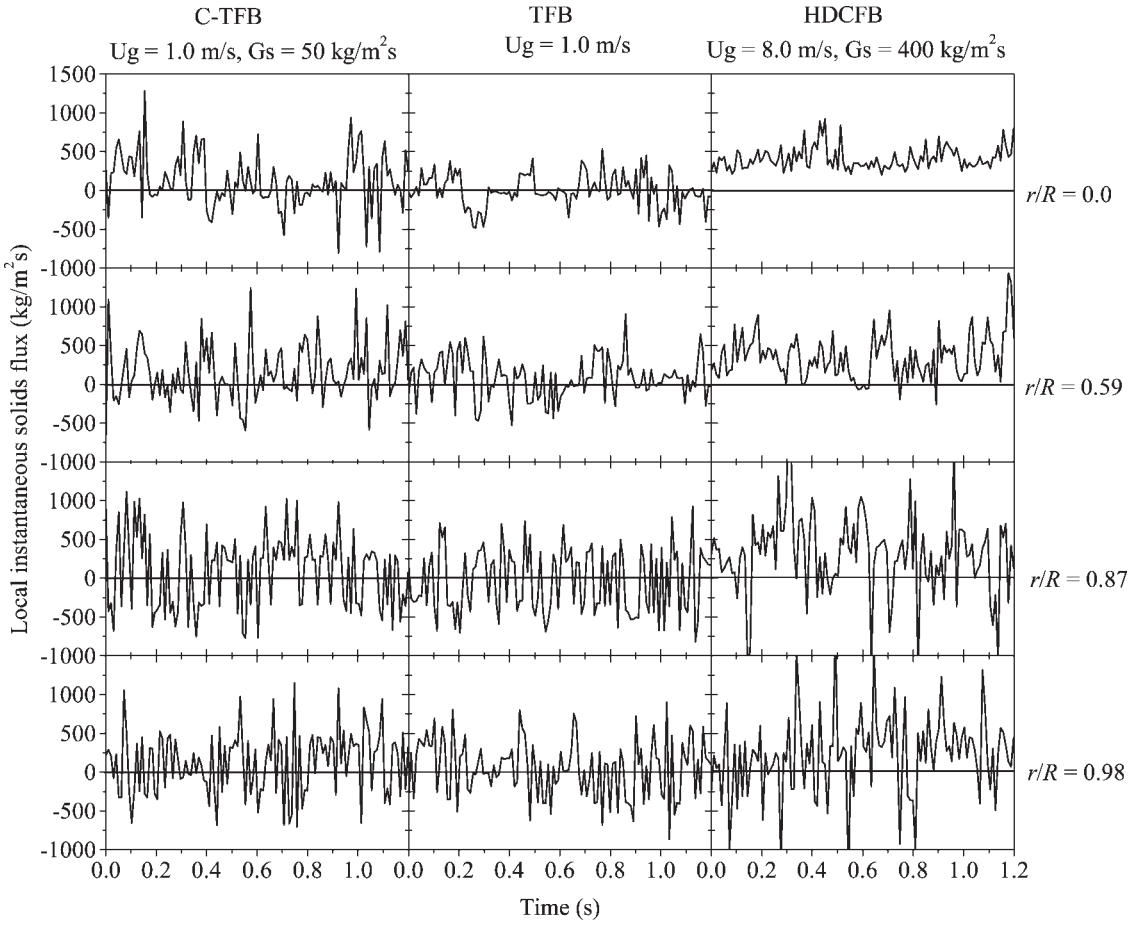

Figure 13. Comparison of instantaneous solids flux in the C-TFB, TFB and HDCFB at the same axial level (z = 0.8 m).

predominate over the gas-particle interactions (drag forces) in the C-TFB, while in the conventional CFB, the movements of the gas-solid suspension are controlled by the drag forces exerted on the particles by the gas. Consequently, the turbulence intensity and frequency in the C-TFB are higher than those in the CFB, resulting in a better gas-solid contacting and heat/mass transfers.

Solids flux standard deviation

The standard deviation of solids flux can quantitatively reflect the turbulent intensity. To this end, Figures 15 and 16 compare the radial profiles of the standard deviation of solids flux in the C-TFB, TFB, HDCFB and CFB on the same axial level, respectively. It can be seen from Figure 15 that the radial profiles of the solids flux standard deviation in the C-TFB, TFB and HDCFB all reach a maximum at some intermediate radial location between the column center and the wall, but the solids flux standard deviations and the radial positions to reach their maxima differ greatly in the C-TFB, TFB, and HDCFB. As shown in Figure 15, the solids flux standard deviations in the center region of the HDCFB are much lower than those in the C-TFB and TFB, while in the wall region, the solids flux standard deviations in the HDCFB are much higher than those in the C-TFB and TFB. Consequently, the radial solids flux standard deviation profile in the HDCFB is less uniform than those in the C-TFB and TFB, unfavorable for uniform gas-solid contacting and heat/mass transfers across the bed section. Furthermore, within the cross-section of the column, the solids flux standard deviations in the C-TFB are higher than those in the TFB, indicating intenser turbulence of gas-solid transient dynamics in the C-TFB.

As shown in Figure 16, under the same operating condition, the solids flux standard deviations in the C-TFB are remarkably higher than those in the CFB; furthermore, the radial distribution of the solids flux standard deviations in the C-TFB is also more uniform than that in the CFB. This indicates that the turbulence of gas-solid suspension flow in the C-TFB is much more vigorous than that in the CFB due to the higher-solids concentration, and then significantly increased particle-particle interactions (collisions) in the C-TFB. The strong fluctuations of solids fluxes in the C-TFB result in excellent contacting and mixing, as well as heat/mass transfer between the gas and solid phases.

Zhu and Zhu[19] also compared the radial profiles of local time-mean net solids flux in the TFB, C-TFB and HDCFB. Their results confirmed that a fairly uniform radial solids flux distribution with no net downward solids flux in the C-TFB, compared with the significant radial nonuniformity of solids flux in the HDCFB, and with the internal recycle of solids flow in the TFB.

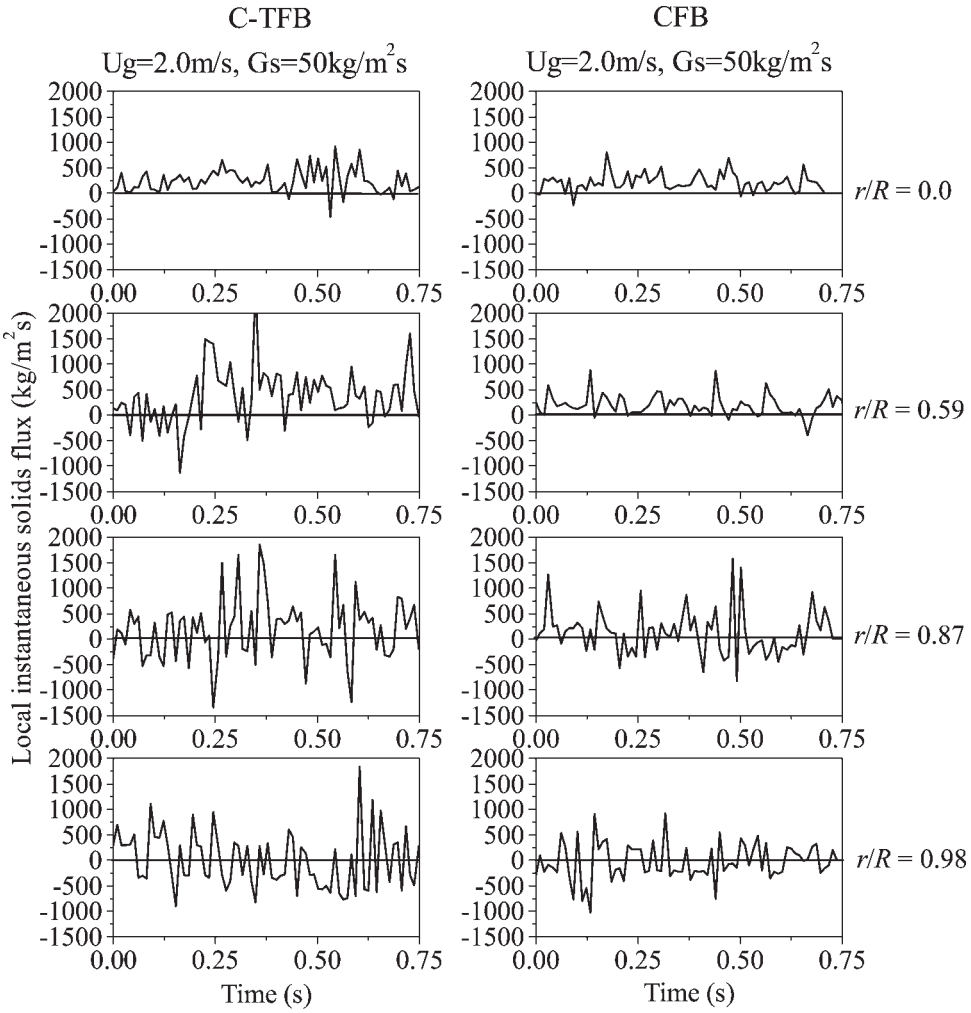

Figure 14. Comparison of instantaneous solids flux in the C-TFB and CFB at the same operating condition and axial level (z = 1.5 m).

Circulating turbulent fluidization regime

As discussed previously and reported by Zhu and Zhu,[18,19] the macro-and microflow structure inside the C-TFB is shown many unique features substantially different than those in the TFB, HDCFB and CFB. Clearly, the operation inside the C-TFB cannot be applicable of the flow regime in the TFB, HDCFB and CFB, since there are some key features in the C-TFB which differ from their respective intrinsic properties of the operations. Given the vigorous particle-particle interactions enabled by high solids concentrations, as well as low-gas velocities, and the high-back pressure at the bottom of the C-TFB provided by the downcomer with high-solids level, the newly designed C-TFB can be operated completely beyond the typical type B or C choking conditions,[43] and the saturation carrying capacity of the corresponding gas velocity.[44] For example, according to Bai and Kato,[44] the saturation carrying capacity for a gas velocity of 1.0 m/s for FCC particles is only 20 kg/m^{2}s. While in the C-TFB, at the superficial gas velocity of 1.0 m/s, a typical operating gas velocity in the C-TFB, the solids circulation rates can easily reach 150 kg/m^{2}s or even higher, well beyond the

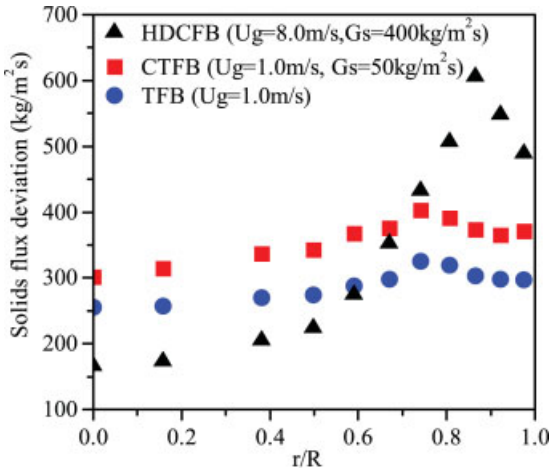

Figure 15. Comparison of solids flux fluctuation in the C-TFB, TFB and HDCFB at the same axial level (z = 0.8 m).

[Color figure can be viewed in the online issue, which is available at www.interscience.wiley.com.]

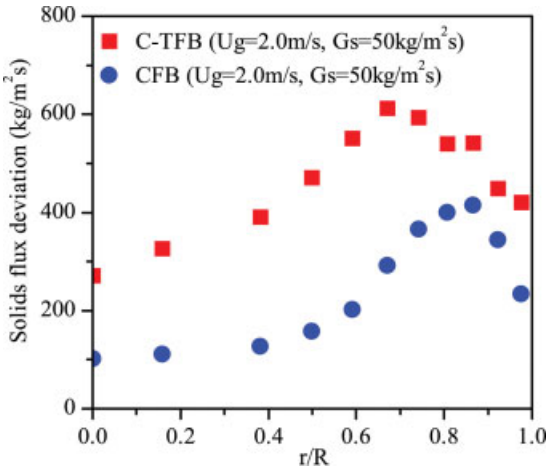

Figure 16. Comparison of solids flux fluctuation in the C-TFB and CFB at the same operating condition and axial level (z = 1.5 m).

[Color figure can be viewed in the online issue, which is available at www.interscience.wiley.com.]

corresponding saturation carrying capacity. Also, the superficial gas velocity of 2.0 m/s, another typical operating gas velocity in the C-TFB, is beyond the upper limit of the operating gas velocity of "regular" turbulent fluidized beds. In addition, for the FCC particles used in this study, the significant entrainment velocity U_{tr}, which marks the onset of fast fluidization, is predicted as 1.31 m/s, 1.63 m/s and 1.37 m/s by Bai et al.[45], Bi and Fan[46] and Bi and Grace[47], respectively. Evidently, although the typical gas velocity of 1.0 m/s in the C-TFB is below the aforementioned significant entrainment velocities, the external solids circulation rates in the C-TFB can be as high as 150kg/m^{2}s, which is not a typical condition for fast fluidization. Furthermore, for the solids-circulation rate of 150 kg/m^{2}s with the FCC particles, Grace et al.[8] predicted an onset velocity of 3.79 m/s for the dense suspension flow, which is significantly higher than the typical operating gas velocities (~1-2 m/s) in the C-TFB to sustain the same solids circulation rate.

Consequently, the flow structure inside the circulating turbulent fluidized bed gives rise to a new flow regime, distinctively different from the "regular" turbulent fluidization, fast fluidization and dense suspension upflow regimes. This new flow regime can be termed as *Circulating Turbulent Fluidization regime*. This new flow regime is characterized with (1) no net downflow of solids across the entire column, (2) high overall solids volume concentration of 20–35%, (3) uniform axial flow and relatively uniform radial flow structure, and (4) particle motion dictated more by particle-particle interaction than gas-particle interaction. Clearly, the flow regime of circulating-turbulent fluidization as described previously is capable of meeting the three distinguishing criteria to demarcate a new flow regime from others as suggested by Grace et al.[8]

(1) Circulating turbulent fluidization regime has *distinctive features*: circulating turbulent fluidization is distinguished from the "regular" turbulent fluidization by nearly no backmixing of solids, as well as high-solids concentration, from dense suspension upflow by particle motion dominated by particle-particle interactions (collisions), and much narrower solids residence time-distribution, and from fast fluidization by much higher suspension density and much more uniform axial and radial flow structure.

(2) Circulating turbulent fluidization regime also has *distinctive trends*. That is, within the operating conditions of C-TFB, gas-particle interactions and particle-particle interactions, axial and radial profiles of solids concentration and particle velocity, and gas and solids backmixing, all show some unique trends which differ from those in other flow regimes.

(3) Axial profiles of solids concentration by Zhu and Zhu[18] indicate that *fully developed* conditions and *statistically steady* can be achieved under circulating turbulent fluidization conditions, provided that the column is tall enough.

Based on the above experimental results and those reported by other researchers (e.g., Rodes et al.[48,49]; Issangya et al.[13–15]; Bai et al.[50]; Grace et al.[8]; Grace[5]; Bi et al.[7,17]; Du et al.[9,51]; Zhu and Zhu[18,19]), key features of the flow behavior inside the C-TFB can be summarized in Table 1, together with those of other "neighboring" flow regime: "regular" turbulent fluidization, fast fluidization and dense suspension upflow. Significant differences can be seen between the flow behaviors of the C-TFB and those of TFBs, CFBs and HDCFBs.

Compared with "regular" turbulent fluidization regime, circulating-turbulent fluidization regime has two key intrinsically different features: nearly no solids backmixing and high-external solids circulation, while other features of circulating turbulent fluidization are almost the same as those of "regular" turbulent fluidization. The characteristics of particle-particle interactions in circulating turbulent fluidization are essentially similar to those of "regular" turbulent fluidization, but are totally different from those observed in fast fluidization and dense suspension upflow. These make the operation of circulating turbulent fluidization advantageous for catalytic reactions where relatively uniform gas and solids residence times, fast deactivation and regeneration of catalyst particles, and good mass/heat transfers are required.

Although there are significant similarities between the operation mode of circulating-turbulent fluidization and dense suspension upflow, as shown in Table 1, the key feature of particle motion in the two regimes are different. It is this difference in particle motion characteristic that distinguishes circulating turbulent fluidization from dense suspension upflow. Also, a broad gas and solids residence-time distribution, resulting from the nonuniform radial flow structure of dense suspension upflow, makes the operation of dense suspension upflow disadvantageous for reactions where uniform gas-solid contact time and high selectivity are required, even though the operation mode of dense suspension upflow has many useful properties such as high-reaction intensity, nearly no backmixing, high external solids circulation, and independent gas and solids residence-time control.

In comparison to the flow regime of fast fluidization, the operation of circulating-turbulent fluidization has the same advantages as those of fast fluidization, such as continuous operation, coupled with high-gas and solids throughput, independent gas and solids residence time-control are favorable for reactions. However, the circulating turbulent fluidization

Table 1. Key Features of High-Velocity Gas-Solid Fluidization Regimes for Group A Particles

Flow Regime	Turbulent fluidization	Circulating turbulent fluidization	Dense suspension upflow	Fast fluidization
Typical superficial gas velocity (m/s)	~0.5-1.5	~1-3	~6-10	~3-8
Typical solids circulation rate ($kg/m^2 \cdot s$)	–	~50-500	~300-1000	<200
Overall solids concentration (%)	~25-35	~20-30	~10-20	~0.3-10
Backmixing	Severe solids backmixng, some gas backmixing	Nearly no solids backmixing, limited gas backmixing	Some limited solids backmixing, limited gas backmixing	Serious solids backmixing, reduced gas backmixing
Reaction intensity (1=lowest, 5=highest)	4	5	3	2
Direction of particle motion at wall	Almost all downward	Mostly upward	Mostly upward	Mostly downward
Uniformity	Uniform axial flow structure, nearly uniform radial flow structure	Uniform axial flow structure, fairly uniform radial structure	Uniform axial flow structure, non-uniform radial flow structure	Non-uniform axial and, radial flow structure
Particle motion	Particle-particle interaction dominating	Particle-particle interaction dominating	Gas-particle interaction dominating	Gas-particle interaction dominating

regime overcomes the two key disadvantages of fast fluidization: low-solids concentration and extremely nonuniform flow structure, characterized by S or exponential shape profile in the axial direction, and core-annulus flow structure in the radial direction, resulting in low-gross reaction intensity, low bed-to-surface heat transfer efficiency, and serious backmixing of solids. Obviously, the operation of circulating turbulent fluidization maintains such advantages of fast fluidization, while avoids the disadvantages of fast fluidization by increasing solids concentrations and uniformity of flow structure.

Furthermore, regime transitions from circulating turbulent fluidization to other "neighboring" flow regimes can also be seen from Table 1. From typical operation conditions of circulating-turbulent fluidization, a regime transition to "regular" turbulent fluidization can occur when decreasing superficial gas velocity and cancelling the secondary air supply; and a regime transition may occur when increasing superficial gas velocity and cancelling the secondary air supply. Circulating-turbulent fluidization can transit to dense suspension upflow when increasing superficial gas velocity and further increasing solids circulation rate from typical operation conditions of circulating turbulent fluidization.

In essence, C-TFB can maintain a high-solids concentration to intensify gas-solids contact efficiency and to enhance chemical reaction while suppress axial solids backmixing to accommodate reactions where a narrow solids residence-time distribution is required for high selectivity. For example, C-TFB is especially useful for gas-phase catalytic reactions, where particulate catalysts deactivate fairly quickly, and, therefore, require continuous regeneration. In this case, C-TFB restrains axial solids backmixing to ensure uniform gas-solid contact time (a feature of CFB) and high gas-solid contact efficiency (a feature of regular turbulent fluidized bed). In other words, C-TFB combines both benefits of TFB and CFB at the same time. More benefits of C-TFB can be further revealed after more quantitative studies on flow behaviors, such as gas and particle mixing and mass/heat transfers are carried out. In addition, the boundaries that demarcate the flow regime of circulating turbulent fluidization from the "regular" turbulent fluidization, fast fluidization and dense suspension upflow are also needed to be completely identified

Conclusions

This work presented in-depth investigation into the transient flow behaviors in a novel C-TFB, featured by low superficial gas velocities and high-solids circulation rates, using a novel multi-functional optical fiber probe which is capable of simultaneously and instantaneously measuring local solids concentrations and particle velocities. Microhydrodynamic distinctions between the gas-solid suspensions in the C-TFB, TFB, CFB and HDCFB were also intensively studied. The experimental results show:

(1) Significant nonuniform radial distribution of solids concentrations and particle velocities in the CFB and HDCFB, leads to much more segregation of the gas-phase from the solids-phase in radial direction than that in the C-TFB and TFB, resulting in a broader residence-time distribution of gas and solid phases and less gas-solid contacting. Uniform radial distribution of the solids concentrations and particle velocities with no net downflowing particles in the C-TFB is one of the key advantages of C-TFBs over conventional CFBs and HDCFBs.

(2) Although the radial profiles of solids concentration and particle velocity in the C-TFB are nearly close to those in the TFB at the same superficial gas velocity, turbulence intensity and frequency in the C-TFB are greater than those in the TFB at the same superficial gas velocity, due to significant external solids circulation and intenser particle-particle interactions.

(3) A random flow structure is observed in the C-TFB. Particle-particle interactions (collisions) dominate the motion of particles in the C-TFB and TFB, totally different from the interaction mechanism between the gas and solid phases in the conventional CFB and the HDCFB, where the movements of particles are mainly controlled by the gas-particle interactions (drag forces).

As a result, the circulating-turbulent fluidization is a new flow regime, independent of turbulent fluidization, fast fluid-

ization and dense suspension upflow. The flow behavior in the C-TFB has its inherent characteristics, different from those in the CFB, TFB and HDCFB reactors. This novel C-TFB reactor is an attractive new reactor with high conversions and/or selectivities, as well as excellent heat/mass transfer and mixing of gas and solids.

Acknowledgments

The authors are grateful to the Natural Science and Engineering Research Council of Canada for financial support.

Notation

D = riser internal diameter, mm
d_p = Sauter mean diameter of particles, μm
G_s = solids circulation rate, kg/m^2·s
G_s* = integrate local net solids fluxes across the riser cross-section, kg/m^2·s
$G_s(t)$ = instantaneous solids flux, kg/m^2·s
L_c = effective distance between the two subprobes, m
r = radial coordinate, m
r/R = normalized radial distance from the riser center
R = riser radius, m
T_{AB} = time shift, s
T_d = integration period of time, s
t = time, s
U_g = superficial gas velocity, m/s
U_{tr} = onset gas velocity of fast fluidization, m/s
V_p = time-mean particle velocity, m/s
$V_p(t)$ = instantaneous particle velocity, m/s
z = axial position from the riser gas distributor, m

Greek letters

ε_s = local time-mean solids holdup
$\varepsilon_s(t)$ = instantaneous solids concentration
$\bar{\varepsilon}_s(t)$ = instantaneous time-averaged solids concentration within the integration time period
ρ_p = particle density, kg/m^3

Literature Cited

1. Kunii D, Levenspiel O. *Fluidization Engineering*, London: Butterworth-Heinmann; 1991.
2. Grace JR, Bi HT. Introduction to circulating fluidized beds. In: Grace JR, Avidan AA, Knowlton TM, eds. *Circulating Fluidized Beds*, London: Chapman & Hall; 1997:1–18.
3. Grace JR, Bi HT, Golriz M. Circulating Fluidized Beds. In: Yang WC eds. *Handbook of Fluidization and Fluid-Particle Systems*. New York: Marcel Dekker; 2003:485–544.
4. Johnsson F. Fluidized bed combustion for clean energy. in: Bi HT, Berruti F, Pugsley T, eds. *Fluidization XII*. Vancouver: Engineering Foundation; 2007:47–62.
5. Grace JR. Reflections on turbulent fluidization and dense suspension upflow. *Powder Technol*. 2000;113:242–248.
6. Lim KS, Zhu JX, Grace JR. Hydrodynamics of gas-solid fluidization. *Intl J Multiphase Flow*. 1995;21(suppl.):141–193.
7. Bi HT, Ellis N, Abba IA, Grace JR. A state-of-the-art review of gas-solid turbulent fluidization. *Chem Eng Sci*. 2000;55:4789–4825.
8. Grace JR, Issangya AS, Bai DR, Bi HT, Zhu JX. Situating the high-density circulating fluidized bed. *AIChE J*. 1999;45:2108–2116.
9. Du B, Warsito W, Fan LS. Bed nonhomogeneity in turbulent gas-solid fluidization. *AIChE J*. 2003;49:1109–1126.
10. Zhu JX. Circulating fluidized beds - recent developments and research requirements in the near future. In: Cen K, eds. *CFB VIII*. Hangzhou: International Academic Publishers; 2005:41–55.
11. Dry RJ, Christensen IN, White CC. Gas-solids contact efficiency in a High-velocity fluidised bed. *Powder Technol*. 1987;52:243–250.
12. Bi HT, Zhu JX. Static instability analysis of circulating fluidized beds and concept of high-density risers. *AIChE J*. 1993;39:1272–1280.
13. Issangya AS, Bai DR, Grace JR, Zhu JX. Solids flux profiles in a high-density circulating fluidized bed riser. In: Fan LS, Knowlton TM, eds. *Fluidization IX*. New York: Engineering Foundation; 1998:197–204.
14. Issangya AS, Bai DR, Bi HT, Lim KS, Zhu JX, Grace JR. Suspension densities in a high-density circulating fluidized bed riser. *Chem Eng Sci*. 1999;54:5451–5460.
15. Issangya AS, Grace JR, Bai DR, Zhu JX. Further measurements of flow dynamics in a high-density circulating fluidized bed riser. *Powder Technol*. 2000;111:104–113.
16. Liu JZ, Grace JR, Bi HT, Morikawa H, Zhu JX. Gas dispersion in fast fluidization and dense suspension upflow. *Chem Eng Sci*. 1999;54(22):5441–5449.
17. Bi HT. Gas and solid mixing in high-density CFB risers. *Int J Chem Reactor Eng*. 2004;2:A12.
18. Zhu HY, Zhu JX. Gas-solids flow structures in a novel circulating-turbulent fluidized bed. *AIChE J*. 2008;54(5):1212–1223.
19. Zhu HY, Zhu JX. Comparative study of flow structures in a circulating-turbulent fluidized bed. *Chem Eng Sci*. 2008;63:2920–2927.
20. Park A, Bi HT, Grace JR. Reduction of electrostatic charges in fluidized beds. *Chem Eng Sci*. 2002;57:153–162.
21. Herbert PM, Gauthier TA, Briens CL, Bergougnou MA. Application of fiber optic reflection probes to the measurement of local particle-velocity and concentration in gas-solid flow. *Powder Technol*. 1994; 80:243–252.
22. Johnsson H, Johnsson F. Measurements of local solids volume-fraction in fluidized bed boilers. *Powder Technol*. 2001;115:13–26.
23. Liu JZ, Grace JG, Bi HT. Novel multifunctional optical-fiber probe: development and validation. *AIChE J*. 2003;49(6):1405–1420.
24. Liu JZ, Grace JG, Bi HT. Novel multifunctional optical-fiber probe: high-density CFB measurements. *AIChE J*. 2003;49(6):1421–1432.
25. Ellis N, Bi HT, Lim CJ, Grace JR. Influence of probe scale and analysis method on measured hydrodynamic properties of gas-fluidized beds. *Chem Eng Sci*. 2004;59(8–9):1841–1851.
26. Zhang H, Johnston PM, Zhu JX, de Lasa HI, Bergougnou MA. A novel calibration procedure for a fiber optic solids concentration probe. *Powder Technol*. 1998;100:260–272.
27. van Ommen JR, Mudde RF. Measuring the gas-solids distribution in Fluidized beds - a review. in: Bi HT, Berruti F, Pugsley T, eds. *Fluidization XII*. Vancouver: Engineering Foundation; 2007:31–46.
28. Werther J. Measurement techniques in fluidized beds. *Powder Technol*. 1999;102:15–36.
29. Cui HP, Mostoufi N, Chaouki J. Characterization of dynamic gas-solid distribution in fluidized beds. *Chem Eng J*. 2000;79:133–143.
30. Li J, Kuipers AM. Effect of competition between particle-particle and gas-particle interactions on flow patterns in dense gas-fluidized beds. *Chem Eng Sci*. 2007;62:3429–3442.
31. van der Stappen MLM, Schouten JC, van den Bleek CM. Deterministic chaos analysis of the dynamical behavior of slugging and bubbling fluidized beds. In: *Proceedings of the 12th Fluidized Bed Combustion*. New York: ASME; 1993:129–140.
32. Lin Q, Wei F, Jin Y. Transient density signal analysis and two-phase micro-structure flow in gas-solids fluidization. *Chem Eng Sci*. 2001;56:2179–2189.
33. Malcus S, Chaplin G, Pugsley T. The hydrodynamics of the high-density bottom zone in a CFB riser analyzed by means of electrical capacitance tomography (ECT). *Chem Eng Sci*. 2000;55:4129–4138.
34. Brereton CMH, Grace JR. Microstructural aspects of the behavior of circulating fluidized beds. *Chem Eng Sci*. 1993;43:2565–2572.
35. Parssinen JH, Zhu JX. Particle velocity and flow development in a long and high-flux circulating fluidized bed riser. *Chem Eng Sci*. 2001;56(18):5295–5303.
36. Yan AJ, Zhu JX. Scale-up effect of riser reactors - particle velocity and flow development. *AIChE J*. 2005;51(11):2956–2964.
37. Bao J, van de Wall RE and Soo S.L. Simultaneous use of LDV and PDPA on particle suspensions. In: Kwauk M, Li JH, eds. *CFB V*, Beijing: Science Press; 1996:1–6.
38. Mathiesen V, Solberg T, Hjertager BH. An experimental and computational study of multiphase flow behavior in a circulating fluidized bed. *Int J Multiphase Flow*. 2000;26:387–419.

39. Monceaus L, Azzi M, Molodtsof Y, Large JF. Particle mass flux profiles and flow regime characterization in a pilot-scale fast fluidized bed unit. In: Ostergaard K and Sorensen A, eds. *Fluidization V*, New York: Engineering Foundation; 1986:337–344.
40. Herb B, Dou K, Tuzla K, Chen JC. Solid mass fluxes in circulating fluidized beds. *Powder Technol*. 1992;70:197–205.
41. Wei F, Lu F, Jin Y, Yu ZQ. Mass flux profiles in a high density circulating fluidized bed. *Powder Technol*. 1997;91:189–195.
42. Yan AJ, Zhu JX. Scale-up effect of riser reactors (1) - axial and radial solids concentration distribution and flow development. *Ind Eng Chem Res*. 2004;43(18):5810–5819.
43. Bi HT, Grace JR, Zhu JX. Types of choking in vertical pneumatic systems. *Int J Multiphase Flow*. 1993;19:1077–1092.
44. Bai D, Kato K. Saturation carrying capacity of gas and flow regimes in CFB. *J Chem Eng Jpn*. 1995;28(2):179–185.
45. Bai D, Jin Y and Yu Z. Flow regimes in circulating fluidized beds. *Chem Eng Technol*. 1993;16:307–313.
46. Bi HT and Fan LS. Regime transitions in gas-solid circulating fluidized beds, In: *AIChE Annual Meeting*. Los Angeles; 1991:17–22.
47. Bi HT, Grace JR. Flow regime diagrams for gas-solid fluidization and upward transport. *Int J Multiphase Flow*. 1995;21:1229–1236.
48. Rhodes MJ, Mineo H, Hirama T. Particle motion at the wall of circulating fluidized bed. *Powder Technol*. 1992;70:207–214.
49. Rhodes MJ, Sollaart M, Wang XS. Flow structure in a fast fluid bed. *Powder Technol*. 1998;99:194–200.
50. Bai D, Issangya AS and Grace JR. Characteristics of gas fluidized beds in different flow regimes. *Ind Eng Chem Res*. 1999;38:803–811.
51. Du B, Fan LS, Wei F, Warsito W. Gas and solids mixing in a turbulent fluidized bed. *AIChE J*. 2002;48(9):1896–1909.

Manuscript received Dec. 12, 2007, and revision received Sept. 12, 2008.